Accepted Manuscript

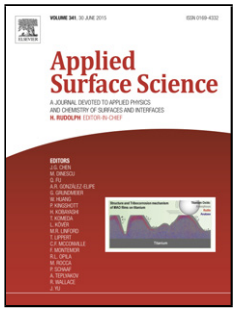

Title: CoPt/TiN films nanopatterned by RF plasma etching towards dot-patterned magnetic media

Authors: János Szívós, Szilárd Pothorszky, Jan Soltys, Miklós Serényi, Hongyu An, Tenghua Gao, András Deák, Ji Shi, György Sáfrán

PII: S0169-4332(17)33305-6
DOI: https://doi.org/10.1016/j.apsusc.2017.11.062
Reference: APSUSC 37644

To appear in: *APSUSC*

Received date: 23-6-2017
Revised date: 27-10-2017
Accepted date: 8-11-2017

Please cite this article as: Szívós J, Pothorszky S, Soltys J, Serényi M, An H, Gao T, Deák A, Shi J, Sáfrán G, CoPt/TiN films nanopatterned by RF plasma etching towards dot-patterned magnetic media, *Applied Surface Science* (2010), https://doi.org/10.1016/j.apsusc.2017.11.062

Elsevier Editorial System(tm) for Applied Surface Science

Manuscript Draft

Manuscript Number: APSUSC-D-17-06440R1

Title: CoPt/TiN films nanopatterned by RF plasma etching towards dot-patterned magnetic media

Article Type: Full Length Article

Keywords: nanopatterning; Langmuir-Blodgett film; RF plasma etching; ordered nanostructures; ferromagnetic thin films

Corresponding Author: Dr. János Szívós,

Corresponding Author's Institution: Institute of Technical Physics and Materials Science, HAS

First Author: János Szívós

Order of Authors: János Szívós; Szilárd Pothorszky; Jan Soltys, PhD; Miklós Serényi, DSc; Hongyu An, PhD; Tenghua Gao; András Deák, PhD; Ji Shi, PhD; György Sáfrán

Cover letter to the manuscript titled "CoPt/TiN films nanopatterned by RF plasma etching towards dot-patterned magnetic media"

Corresponding author: János Szívós. Institute: Institute for Technical Physics and Materials Science, Centre for Energy Research, Hungarian Academy of Sciences. Mailing address: H–1121 Budapest, Konkoly-Thege M. út 29–33. E-mail: szivos.janos@energia.mta.hu, phone: +36-1-392-2222/1876.

Other authors: Szilárd Pothorszky, Jan Soltys, Miklós Serényi, Hongyu An, Tenghua Gao, András Deák, Ji Shi, György Sáfrán.

Applied Surface Science is in a focus of many chemists, engineers, physicists and biologists who work on the field of nanoscale science and nanotechnology. Our paper is appropriate for *Applied Surface Science*, because a novel and general (applicable to wide variety of material surfaces and thin films) nanopatterning technique proposed by the authors eariler, is applied here to successfully fabricate dot-patterned CoPt thin films exhibiting perpendicular magnetism. The manuscript topic fits nicely to the accommodated topics as it deals with 2D assembly and nanopatterning of sputter deposited magnetic CoPt thin films. Our results can be considered as a possibility to realize Bit Patterned Media (BPM). Thus, our paper should be of service for researchers interested in fabricating ordered nanopatterns, in particular perpendicular magnetic dot-patterned thin films. Moreover, the technique applied in this paper can easily be scaled to industrial throughput and it is relatively cheap.

Highlights

- A novel nanopatterning technique proposed recently is applied to CoPt thin films
- CoPt films are transformed to $L1_0$ structure both before and after nanopatterning
- Dot-patterned CoPt films with surface-perpendicular magnetic easy axis were obtained
- Feature size can be reduced to <20nm and possible to scale to industrial throughput
- Our work can be considered as a possibility to realize Bit Patterned Media (BPM)

Responses to the Editor and Reviewers

Editor:

The authors thank to Editor for the remarks. The format of the citations is changed to show all the authors and some more citations towards Applied Surface Science are added to the manuscript. The XRD scales in Figure 4 are corrected as well.

Reviewer #1:

The authors are thankful to Reviewer #1 for the useful comments and remarks. Here are our answers point-by-point:

1) Magnetic properties of the continues film is missing in current manuscript. I suggest add the in-plane and out-of-plane M-H loop to Fig. 8(a). So that the effect of dot geometry can be clearly observed.

The magnetic properties of the annealed but non-patterned CoPt films are described in the authors' previous paper [1]. However, this fact was not mentioned in the in the "magnetic properties" section of the current manuscript. The previous paper was only cited in other sections of the current manuscript. For comparison, the VSM result of an annealed but non-patterned CoPt film from our previous paper [1] is shown here together with the VSM Fig. 8(a) from the current manuscript.

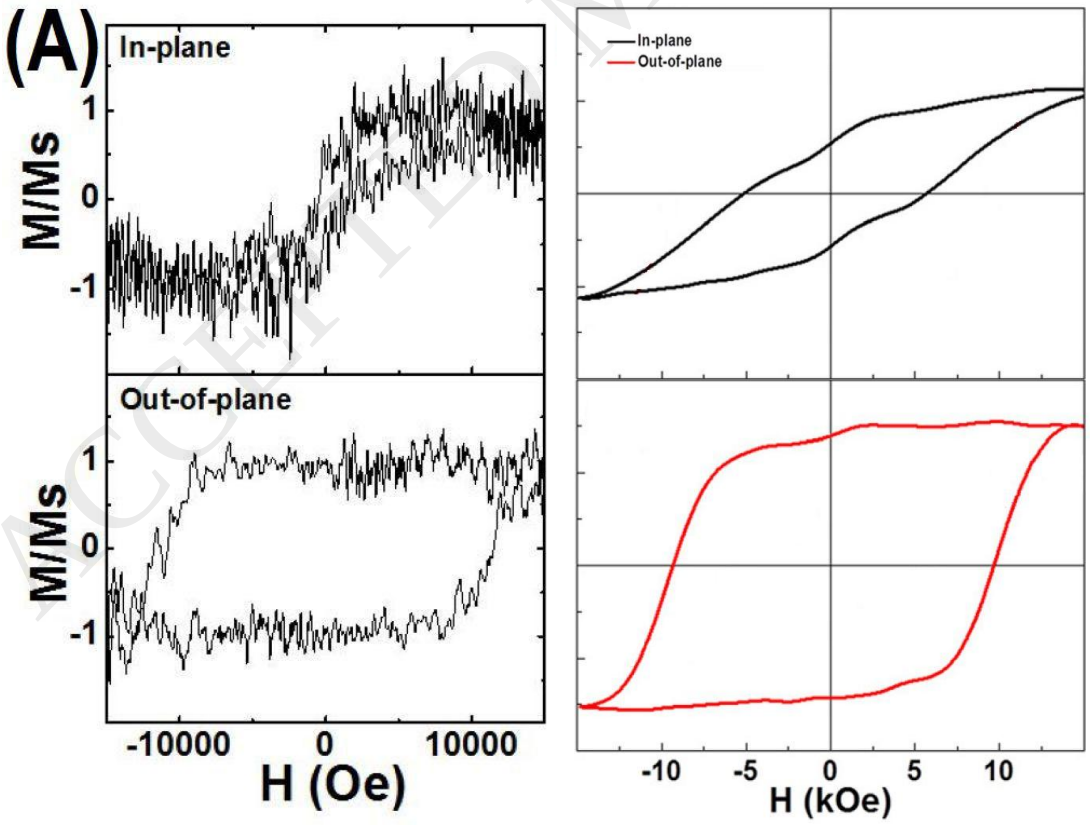

As it is seen, the two perpendicular measurements are very similar (besides the noise). The coercive force of the patterned sample seems to be somewhat larger, but this can't be stated due to the noise of the measurement. On the other hand, the in-plane hysteresis loop is way smaller in the case of the patterned sample. A few words about this comparison are added to the "magnetic properties section" of the current manuscript together with a citation to our previous paper.

2) It will be good also compare the M-H loop before and after annealing. For both dot array and continuous film.

For comparison, the Fig 8(a) of the manuscript can be seen below together with a VSM taken from a dot-patterned but non-annealed CoPt film.

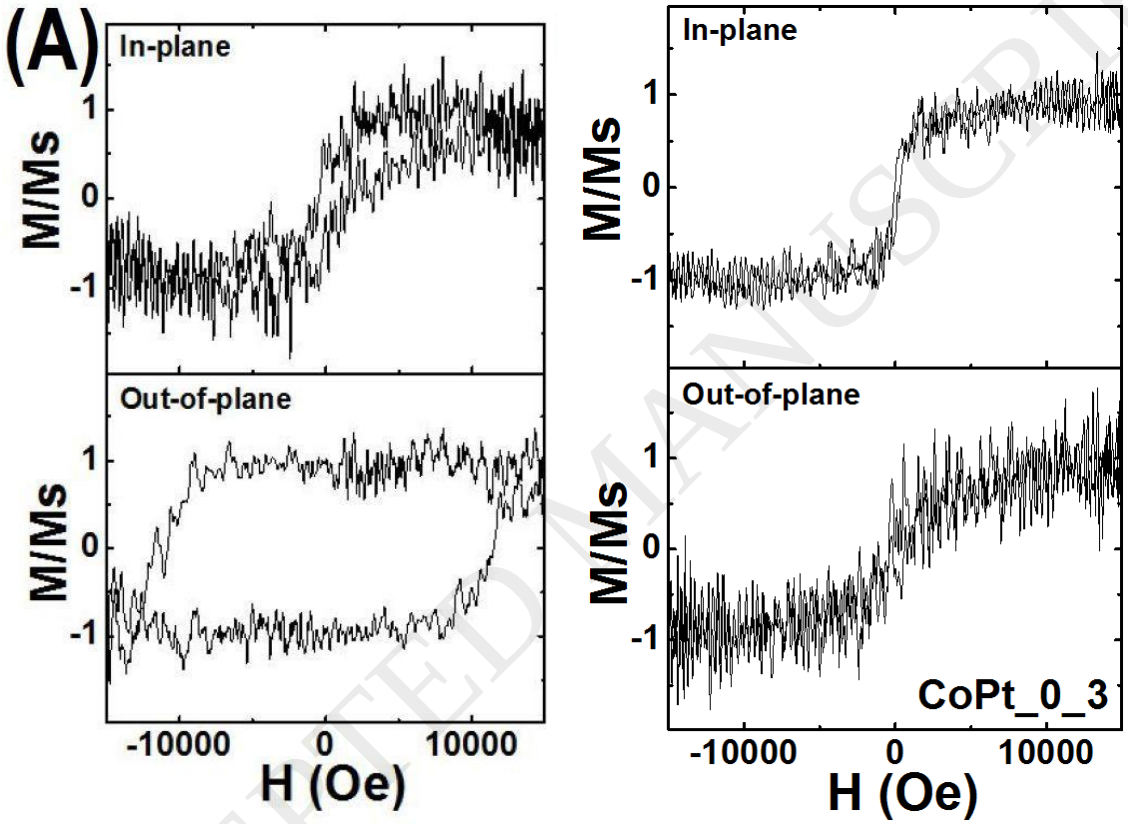

As it is seen, the patterned but non-annealed CoPt film doesn't show significant hysteresis neither in plane nor out of plane direction. This is due to the disordered fcc phase; there is no macroscopic anisotropy. Of course, this latter holds for the non-patterned and non-annealed case as well. Furthermore, the magnetic behaviour of the continuous CoPt films can be found in e. g. [2] or [3]. These comments and the VSM result of the patterned but non-annealed are added to the manuscript.

3) The MFM image of the CoPt dot array is kind of confusing. The MH loop in Fig. 8(a-bottom panel) clearly shows that the magnetization of all dots should be along up or down direction at remanent state. However, the MFM image in Fig. 8(b) is fully random. Please try to provide an MFM image with longer etching time, if the authors think the etching time is too short for this sample.

The authors are thankful for the good remarks. We agree that the saturated sample with well separated dots would exhibit magnetization of all dots either up or down.
We have to clarify the conditions of the MFM measurements in the following. The actual sample pieces used for the MFM measurements are different from those studied by the VSM (but identical in sense of fabrication process).
The sample pieces for the MFM measurements were only magnetized by an available external magnet at various fields in the range of 0T to 1.15T (1.15T is maximum of the available external magnet). The MFM images were taken at directly after this magnetization at zero field. Thus, we strongly suggest that the 1.15 T is not enough to saturate the dot-patterned $L1_0$ CoPt thin films. (E.g. a calculation had shown [4] that the write head has to apply ~2.4 T local field to switch a 1 Tbit/in^2 capacity dot-patterned media.) As a consequence, the MFM images don't show the fully saturated state.
The conditions of the MFM measurements are clarified in the manuscript as well.
Regarding the preparation of new sample etched with longer time, unfortunately, we are not able to realize this experiment within the revision time. The sample from which the MFM images are presented in the article cannot be etched longer as the mask (silica nanospheres) was already removed. So the new experiment would require completing the whole technology from the beginning, i.e. CoPt sputtering, nanopatterning, analysing and MFM measuring.

4) Did the MFM image take after saturating the sample along one direction? MFM image as a function of the magnetic field history may help us to understand the switching process of the array. For example, the switching field in Fig. 8(a-bottom-panel) is around 10500 Oe, MFM image should be different if a magnetic field of 12000, 11000, 10500, 10000 and 9000 is applied to the array. A uniform up magnetization, random magnetization and uniform down magnetization should be observed in the experiment.

This question is strongly correlated to the previous one. As it was mentioned in our previous answer, a number of MFM measurements were performed directly after magnetizing sample at various fields in the range of 0T to 1.15T. However, all MFM scans looks similar to that provided in the manuscript. There is no significant difference between the images obtained in different external fields of this range. As it was detailed above, we suppose that the 1.15 T was not enough to saturate the dot-patterned $L1_0$ CoPt thin films. Therefore, we couldn't observe the "uniform up magnetization, random magnetization and uniform down magnetization" sequence by means of the MFM measurements.
(In theory, it is possible to investigate the switching process of the CoPt array by properly magnetizing a sample prior to the MFM scans by means of the VSM instrument itself. That way, the uniform up magnetization, random magnetization and uniform down magnetization could be observed by the MFM. However, it is unfortunately not likely that such an experiment can successfully be completed by the 30th October (the deadline for revision) due to the workload of responsible co-workers.)

5) There are some minor language mistakes in the manuscript. Please proof read the manuscript and fix them.

The English of the manuscript have been revised; hopefully all the mistakes are eliminated.

6) Please use Fig. 1-a or Fig. 1(a) instead of Fig. 1 a.

The figure citation format is changed to the Fig. 1(a) format.

7) Please make sure show the full name before using the abbreviations. For example: FFT, SAED and so on.

The missing abbreviation definitions are added to the manuscript.

References

[1] Hongyu An et al., "Perpendicular coercivity enhancement of CoPt/TiN films by nitrogen incorporation during deposition," *Journal of Applied Physics*, vol. 118, pp. 203907 1-4, 2015.

[2] Kevin R. Coffey, Michael A. Parker, and J. Kent Howard, "High Anisotropy L10 Thin Films for Longitudinal Recording," *IEEE Transactions on Magnetics*, vol. 31 (6), pp. 2737-2739, 1995.

[3] R. Gontarz, T. Luciński, L. Uba, S. Uba, and Yu. Kudryavtsev, "Annealing Effect of Equiatomic Co/Pt Alloy Films," *Acta Physica Polonica A*, vol. 85 (2), pp. 427-431, 1994.

[4] Sharat Batra, Jonathan D. Hannay, Hong Zhou, and Jason S. Goldberg, "Investigations of perpendicular write head design for 1 Tb/in2," *IEEE transactions on magnetics*, vol. 40 (1), pp. 319-325, 2004.

CoPt/TiN films nanopatterned by RF plasma etching towards dot-patterned magnetic media

János Szívós[a,b,*], *Szilárd Pothorszky*[a], *Jan Soltys*[c], *Miklós Serényi*[a], *Hongyu An*[d], *Tenghua Gao*[d], *András Deák*[a], *Ji Shi*[d], *György Sáfrán*[a]

[a]Institute for Technical Physics and Materials Science, Centre for Nuclear Research, Hungarian Academy of Sciences, H-1121 Budapest, Konkoly-Thege M. út 29–33.

[b]Doctoral School of Molecular- and Nanotechnologies, University of Pannonia, H-8200 Veszprém, Egyetem utca 10.

[c]Institute of Electrical Engineering, Slovak Academy of Sciences, 841 04 Bratislava, Dúbravská cesta 9.

[d]School of Materials and Chemical Technology, Tokyo Institute of Technology, 2-12-1, Ookayama, Meguro-ku, Tokyo 152-8552, Japan

*Corresponding author, e-mail: szivos@energia.mta.hu, phone: +36-1-392-2222/1876

Abstract

CoPt thin films as possible candidates for Bit Patterned magnetic Media (BPM) were prepared and investigated by electron microscopy techniques and magnetic measurements. The structure and morphology of the Direct Current (DC) sputtered films with N incorporation were revealed in both as-prepared and annealed state. Nanopatterning of the samples was carried out by means of Radio Frequency (RF) plasma etching through a Langmuir-Blodgett film of silica nanospheres that is a fast and high throughput technique. As a result, the samples with hexagonally arranged 100 nm

size separated dots of fct-phase CoPt were obtained. The influence of the order of nanopatterning and anneling on the nanostructure formation was revealed. The magnetic properties of the nanopatterned fct CoPt films were investigated by Vibrating Sample Magnetometer (VSM) and Magnetic Force Microscopy (MFM). The results show that CoPt thin film nanopatterned by means of the RF plasma etching technique is promising candidate to a possible realization of BPM. Furthermore, this technique is versatile and suitable for scaling up to technological and industrial applications.

Keywords

nanopatterning; Langmuir-Blodgett film; RF plasma etching; ordered nanostructures; ferromagnetic thin films

1. Introduction

The advancement of nanotechnology is mainly driven by the ability to tailor functional materials on nanoscale. Hence, high research interest is given on the field of nanoscale patterning (i.e. the fabrication of nano-size ordered structures) as well. The technological progress is raising an increasing demand for techniques to prepare large areas of patterned structures with nanoscale precision in a rapid, inexpensive and industrially scalable manner. This applies to the fast growing field of nanopatterning of magnetic materials as well. High-resolution magnetic patterning plays a role in applications like magnetic sensors [1] [2] [3] and actuators [4] [5], spin-electronics or magnonics [6] [7]. Moreover, magnetic nanopattern structures are promising candidates for a qubit realization in quantum informatics [8].

However, the main boost in the progress of the nanopatterning techniques is the development of the Bit Patterned magnetic recording Media (BPM) [9]. BPM is a highly possible approach for overcoming the superparamagnetic limit of current hard drives that originates from the thermally induced magnetic instability due to the high recording density [10]. In the concept of BPM, each recording bit is stored in an individual magnetic dot and so, the inter-dot spacing reduces the interaction between the stored bits that prevents the superparamagnetic transition. In this context, the reduction in the feature size of the nanopattern is required for higher recording densities.

Nowadays, BPM is usually realized by means of a conventional serial patterning technique, e. g. e-beam lithography [11] [12]. The serial methods are precisely controllable, but slow and expensive solutions [13] that cannot be scaled to industrial throughput. Several hybrid possibilities, such as nanoimprint [14] [15] or nanosphere lithography [16] [17] [18] [19] [20] are investigated in order to overcome this issues. The present authors proposed a fast and low cost general technique [21] based on nanosphere lithography that is capable to fabricate sub-100 nm patterns in wide variety of surfaces and thin films. Our method utilizes a monolayer of hexagonally self-assembled silica nanospheres prepared by the Langmuir-Blodgett (LB) technique [22] [23] as a template. The nanopatterning is carried out by RF plasma etching of the sample through a covering LB film [21]. The RF plasma etching is advantageous because, beside metals and semiconductors, it is applicable for etching insulating materials, as well. Thanks to the fact that both LB films and RF plasma can be applied on extended surfaces, our method is suitable to prepare large area of ordered patterns in bulk surfaces and thin films of diverse solids.

In this paper, thin sputter deposited CoPt films of fcc and fct ($L1_0$) structures [24] were patterned by our technique in order to realize ordered nanoscale magnetic dot arrays. The successful preparation of dot-patterned fcc and fct CoPt films was confirmed by Scanning- and (High Resolution) Transmission Electron Microscopy (SEM and (HR)TEM).

Upon annealing, the as-deposited CoPt films undergo a phase transformation from fcc to fct ($L1_0$) structure [24]. It is shown here that the order of the annealing and patterning can be interchanged, the fcc to fct transition may undergo regardless of the order.

In order to reveal the magnetic properties of the nanopatterned fct CoPt films the samples were investigated by Vibrating Sample Magnetometer (VSM) and Magnetic Force Microscopy (MFM).

2. Experimental Methods

A 10 nm thick cobalt-platinum films with 30 nm thick TiN seed layers were DC magnetron sputter deposited onto fused quartz substrates at 400 °C. The base pressure of the vacuum system was below $5*10^{-7}$ mbar, and the sputtering gas was an Ar – N_2 mixture with a deposition pressure of $2*10^{-3}$ mbar. The partial flow rate ($\dot{V}$) ratio of the N_2 (i.e. $\frac{\dot{V}_{N_2}}{\dot{V}_{Ar+N_2}}$) was 0.1 in the case of the TiN seed layer, while it was set to 0.2 for the CoPt deposition. In the former case, a Ti sputtering target of 2” was applied, while that in the latter case was a Co-Pt alloy. The composition of the film was $Co_{0.44}Pt_{0.56}$, measured by inductively coupled plasma-optical emission spectrometer. The thickness of both layers was controlled by the deposition time using a pre-calibrated deposition rate.

Pieces of the as-prepared samples were annealed for 1 h at 700 °C in vacuum, at a pressure below $2.5*10^{-6}$ mbar.

N_2 was incorporated into the CoPt films in order to promote the fcc to $L1_0$ phase transition during annealing [24]. More details of the CoPt sample preparation are described in [24].

The surface of both annealed and as-deposited samples was covered with a monolayer of silica nanospheres self-organized into a hexagonal structure by the LB technique. The 100 nm nominal diameter silica nanospheres and their LB-films were prepared as reported earlier [25] [26] and as it was detailed in [21].

The LB-films were obtained using a KSV 2000 film balance by vertical deposition (5 mm/min) at cca. 80 % of the collapse pressure, which was determined in an earlier experimental run. For the CoPt substrates, the vertical deposition of the LB-film resulted in poor quality monolayers, presumably due to the hydrophobic character of the substrate. The liquid supported LB film could be only partially transferred onto the sample surface. When the substrate inclination was lowered from 90° to 45°, however, a complete monolayer transfer without macroscopic defects was achievable [21].

The CoPt thin film samples covered with the monolayer of silica nanospheres were subjected to Ar plasma-etching in a Leybold Z 400 RF sputter deposition system where the samples were mounted at the target position of the sputtering source. Under such conditions the bombarding Ar-ions impinge the sample surface in the entire half solid angle except in regions and at directions shaded by the silica nanospheres. Thus, with suitably set etching parameters, the silica nanospheres protect the surface and the

sample is etched only in between them. The detailed description of our nanopatterning method can be found in [21].

The base pressure of the sputtering chamber was $6*10^{-6}$ mbar, while the Ar pressure (P_{Ar}) was $2.5*10^{-2}$ mbar during the plasma etching. In order to optimize the pattern obtained, the etching time (t) and the DC wall potential (the DC self-bias potential induced by the RF power, U_{DC}) were varied between 61 and 240 s and 1000-1200 V, respectively. The established power densities (S) are given in the "Results" section in each case. Those were calculated by measuring the ion currents (I_{ion}) and using the target plate (cathode) diameter d_{cat}*=3 in'=7.62 cm*.

Subsequent to plasma etching the LB-films were removed by wiping with cotton wool wetted with acetone.

The surface morphology of the samples was characterized by a LEO 1540 XB Scanning Electron Microscope (SEM) (with Gemini electron optics). The nanostructure of the layers was studied by a 300kV JEOL 3010 (0.17 nm point resolution), and a 200 kV Philips CM 20 (0.27 nm point resolution) Transmission Electron Microscope (TEM). The preparation of the samples for TEM was carried out by mechanical and ion beam thinning. The plan view thinning process was carried out from the back (substrate) side of the sample. An attention was paid not to expose the film surface to any mechanical, nor ion beam treatment.

The magnetic measurements were carried out by a Riken Denshi BHV-50 V Vibrating Sample Magnetometer (VSM) with a maximum magnetic field of 15 kOe; and by a Ntegra Prima Magnetic Force Microscope (MFM).

3. Results and Discussion

3.1. Structure and morphology of the CoPt films

The structure and morphology of the DC magnetron sputtered CoPt films were investigated by SEM, plan view- and cross sectional (X-) TEM. The typical plan view SEM and TEM images of the as-prepared CoPt films are shown in Fig. 1(a) and (b), respectively. The inset is a Selected Area Electron Diffraction (SAED) pattern of the area shown in Fig. 1(b).

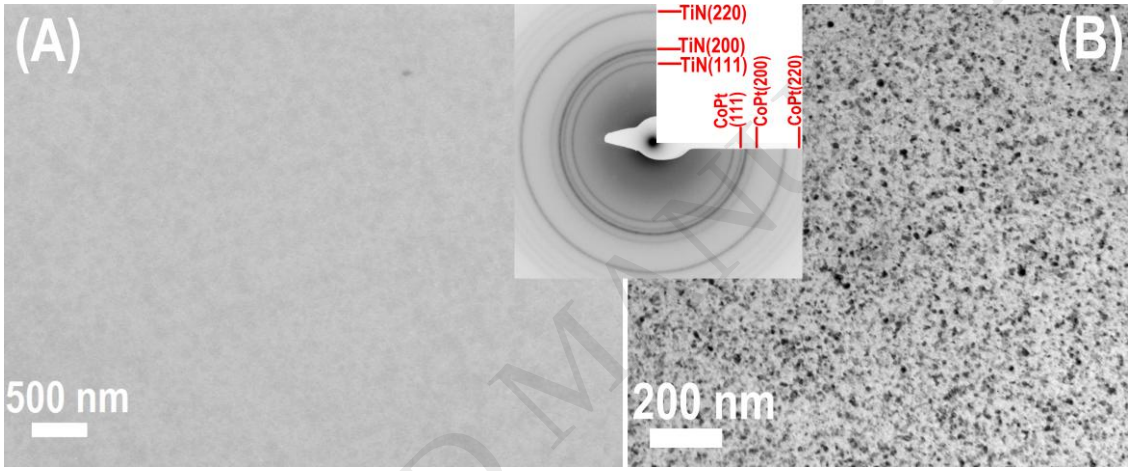

Figure 1. *Plan view SEM (a) and TEM (b) images of the as prepared sample. The SAED inset represents both polycrystalline fcc CoPt and fcc TiN layers.*

The as-prepared films are homogenous, continuous and both TiN and CoPt consist of randomly oriented polycrystalline grains of fcc phase according to the SAED inset. The CoPt and TiN layer consists of crystallites of 10-25 nm lateral size as it is seen in the plan view Bright Field (BF) and Dark Field (DF) TEM images in Fig. 2(a) and (b).

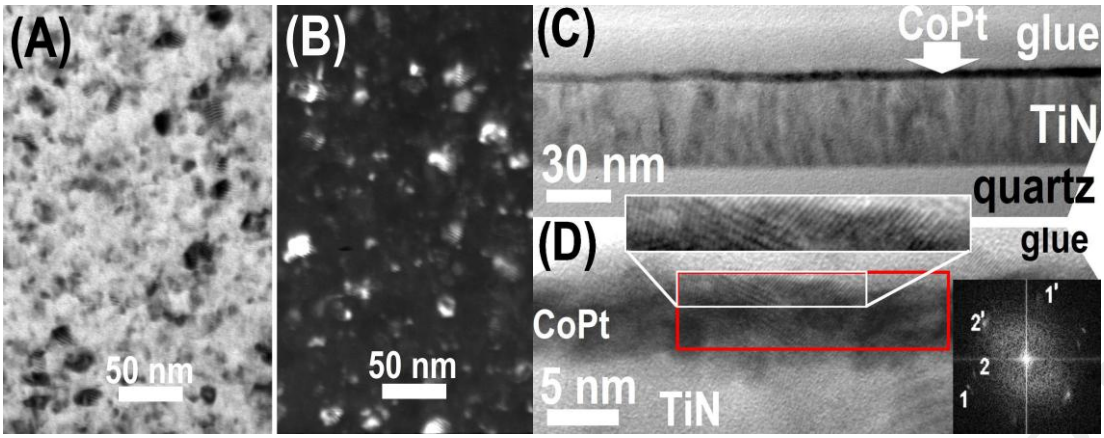

***Figure 2**. Plan view BF (a) and DF (b) TEM, XTEM (c) and HRXTEM (d) images of the as prepared sample. The inset in (d) shows an FFT of the CoPt layer. The numbered reflections in the FFT are: 1 and 1' – CoPt(200); 2 and 2' – CoPt(111). The ROI of the FFT is marked by a (red) rectangle and a part of it is magnified in the inset between (c) and (d).*

Fig. 2(c) depicts the cross-section of the as-prepared films. The thickness of the CoPt layer is found to be 4.8±0.8 nm and that of the TiN layer below is 42.3±1 nm. These values were evaluated from averaging measurements in a couple of XTEM micrographs not shown here. Fig. 2(d) is a High Resolution (HR-) XTEM of the as-prepared CoPt layer with an inset showing the Fast Fourier Transformation (FFT) of image of few CoPt grains. The Region Of Interest (ROI) of the FFT is marked by a (red) rectangle and the upper left part of it (white) is magnified in the inset between Fig. 2(c) and (d) in order to visualize the lattice planes. The CoPt grains can be identified as fcc crystallites by means of the FFT that is in good agreement with the SAED (inset of Fig. 1). In the FFT image, the reflections indicated by 1 and 1' are the CoPt (200) /1.93 Å/, while the reflection 2 and 2' correspond to the CoPt (111) /2.23 Å/ lattice planes. These FFT reflections come from several different crystallites (grains) stacked on each other in the cross-sectional sample.

As it was mentioned in the Experimental, some of the as-prepared samples were annealed at 700 °C in vacuum for 1 h in order to induce the phase transition of the CoPt from fcc to fct. The incorporated N_2 promotes the phase transition that results in a [001]

textured CoPt fct ($L1_0$) phase. This is described in [24], where the typical plan view BF TEM, plan view SAED, cross sectional TEM and HRTEM images of the annealed CoPt samples can be found as well. However, for the complete comparison, the typical (plan view) SEM, SAED and HRXTEM of the annealed samples are included here (Fig. 3).

The annealing doesn't affect the average lateral grain size (~20 nm) remarkably, according to the plan view TEM (not shown here). The SEM image in Fig. 3(a) shows that the surface of the annealed CoPt is not continuous, especially compared to the as-deposited samples. (This is confirmed by the plan view TEM and Atomic Force Microscopy (AFM) results in [24] as well.) Due to annealing, the thickness of the CoPt layer gets fluctuating as it is seen in Fig. 3(c) (and in [24]); its thickness is 7.8±2.6 nm. The thickness of the TiN seed layer, 42.6±1.7 nm, however, remains practically unchanged. The thickness values are averaged data of multiple XTEM micrographs.

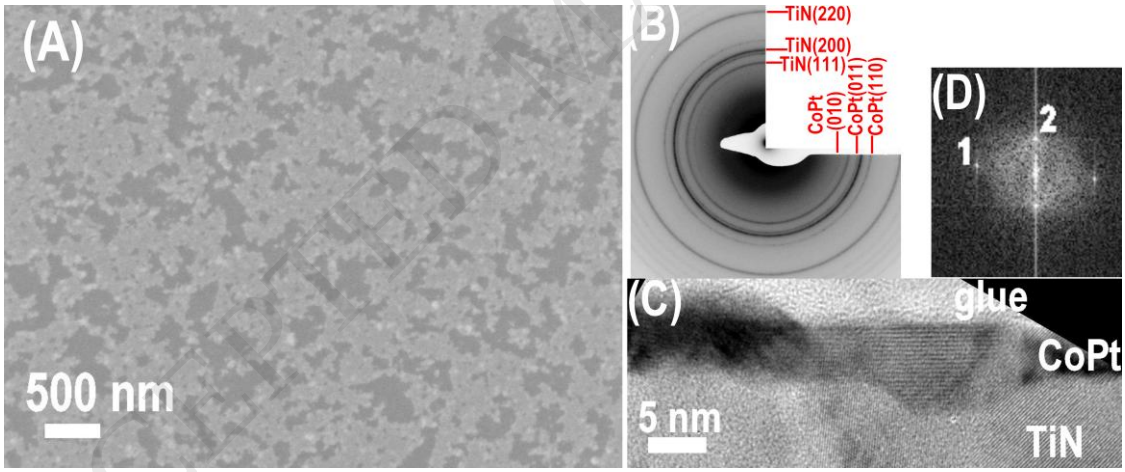

Figure 3. *Plan view SEM (a) and SAED (b) images of the annealed sample. The SAED represents the polycrystalline fct phase CoPt and the fcc TiN layers. The HRXTEM of a typical fct CoPt grain is shown in (c), while (d) is the FFT of the image of CoPt layer in (c). The numbered reflections in the FFT are: 1 – fct CoPt(110); 2 – fctT CoPt(001).*

The typical plan view SAED of the annealed CoPt sample is depicted in Fig. 3(b) that shows the transformed CoPt fct ($L1_0$) phase together with the fcc TiN. It is to mention that, here, the indexing of the fct CoPt rings is different from the one applied in [24].

This is due to the different unit cell selection. In this paper, the conventional primitive cell – P4/mmm space group, a=2.69 Å and c=3.684 Å [27] – was applied as unit cell. The HRXTEM of the annealed CoPt in Fig. 3(c) and in [24] show fct ($L1_0$) phase CoPt grains that confirm the phase-transition. Fig. 3(d) is the FFT of the HR image of the CoPt grain shown in Fig. 3(c); the reflections marked by 1 and 2 correspond to the fct CoPt(110) /1.905 Å/ and fct CoPt(001) /3.684 Å/, respectively. These typical images suggest that the annealed fct CoPt films exhibit preferred [001] orientation.

The intensity distribution of the plan view SAED of the as-prepared and that of the annealed CoPt sample (inset of Fig. 1 and Fig. 3(b)), are depicted in Fig. 4. The bottom (red) graph shows the intensity-distribution corresponding to the as-prepared CoPt sample, while the upper (dark blue) graph is that of the annealed one. The graphs are calibrated by the X-Ray Diffraction (XRD) lines of the fcc TiN [28] that is indicated with the (green) markers named as "FCC TiN" in Fig. 4. Regarding TiN, the intensity of the TiN(200) peak increases while that of the TiN(111) peak decreases due to the annealing according to Fig. 4. This refers to the development a TiN [001] texture. The markers named "FCC CoPt" (blue) and "FCT CoPt" (orange) are associated to the random polycrystalline fcc CoPt and the random polycrystalline fct ($L1_0$) CoPt phases, respectively. These latter two markers were computed by means of the corresponding structure data [29]. As it is seen again from Fig. 4, the as-deposited CoPt (red curve) is polycrystalline fcc that has no texture.

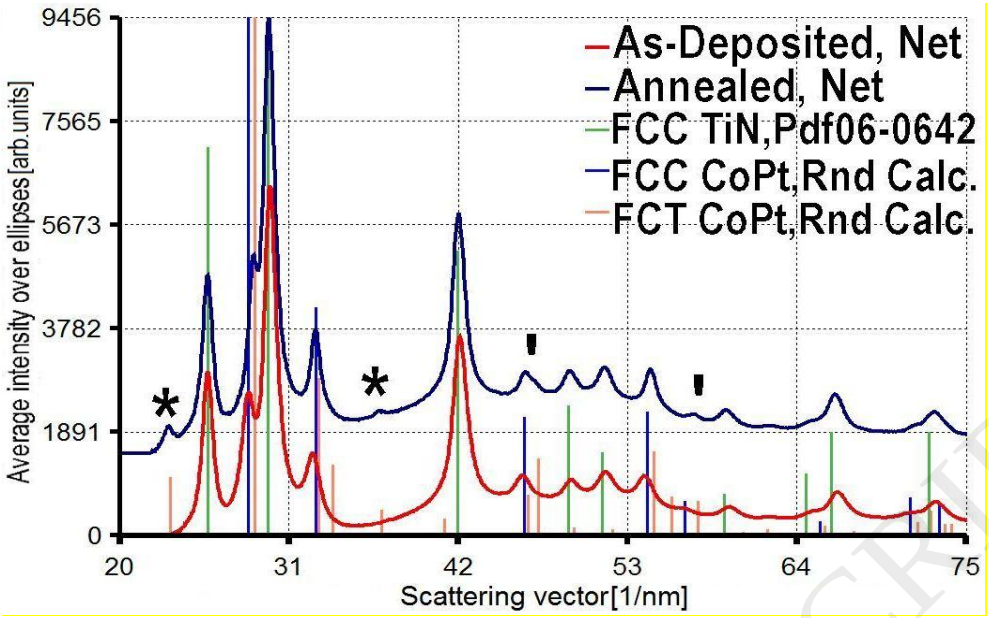

***Figure 4**. The intensity distribution of the typical SAED of the as-deposited (red curve) and of the annealed (blue curve) sample. The calibration was done by means of the TiN markers, and the calculated fcc and fct CoPt markers identify the corresponding phases. For colour version see the electronic release.*

Investigating the upper (dark blue) curve, one can conclude that the annealed CoPt is mostly in polycrystalline fct phase. This is mainly indicated by the appearance of two new peaks which are denoted by "*", they are the fct CoPt(010) and fct CoPt(111) from left to right. However, the presence of the – weak – fct CoPt(111) peak (denoted by the right "*") indicates that the fct CoPt is not completely [001] textured. The two "'" symbols indicate two peaks that have distorted shapes due to a new, partially overlapping peak. This latter suggests that the annealed samples still contain some fcc CoPt grains as well.

The phase analysis in Fig. 4 was assisted by means of J. Lábár's software "Process Diffraction" [30] [31] [32] [33].

3.2. Nanopatterns fabricated in the as-prepared and annealed CoPt samples by RF plasma etching

Both as-prepared and annealed CoPt samples were nanopatterned by means of templating with an LB film of silica nanoballs and RF plasma etching. In the case of the as-prepared CoPt samples, the etching time (t) and the DC wall potential (U_{DC}) were varied between 61 and 220 s and from 1000 to 1200 V. It turned out that the hexagonal pattern of the silica LB film is transferred well into the CoPt layer after only t=100 s at U_{DC}=1000±15V and power density of S=5.85±0.76 W/cm^2. Typical images of an as-prepared CoPt sample treated by using the above settings are depicted in Fig. 5. The SEM micrograph in Fig. 5(a) depicts hexagonally arranged 100 nm size dots. According to the XTEM image in Fig. 5(b) the pattern consists of separated CoPt islands.

It is to mention, that here we used conventional XTEM preparation that cuts the sample at a random azimuth and position with respect to the hexagonal pattern.

On the other hand, the LB films show a domain structure and contain defects that are projected into the CoPt layers. This appears in the SEM images and also in Fig. 5(b) where the red circle marks a small size dot attributed to a defect of the LB film template. It is to mention that there are many efforts to improve the quality of the LB film e.g. [34] [35], however, this issue is beyond the subject of the present study.

We have found that at U_{DC}=1000 V and S=5.85 W/cm^2 the TiN seed layer remains unchanged even after t=220 s etching time. This should be the result of the known hardness and resistance to sputter erosion of TiN [36] [37].

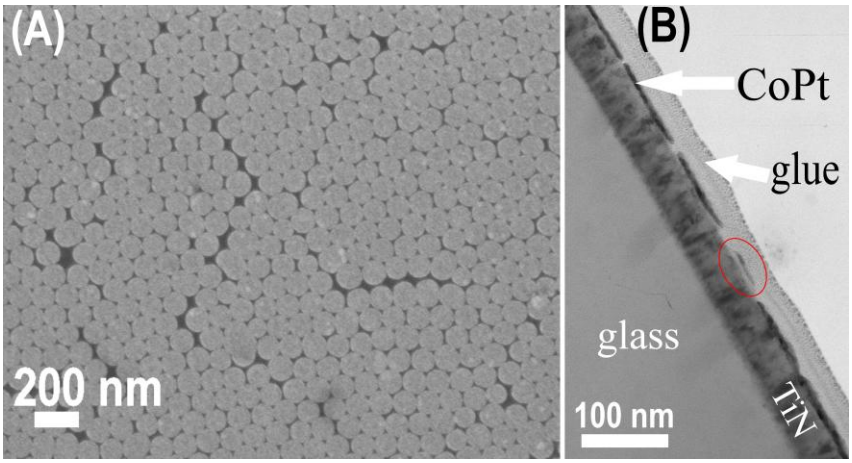

***Figure 5**. SEM (a) and XTEM (b) image of the patterned as-prepared CoPt sample. The etching time was 100 s and U_{DC} was 1000 V. The red ellipse marks a disk from one row back that corresponds to the imaging of a point defect of the LB film.*

It was assumed that the sputtering speed of the annealed ($L1_0$ phase) CoPt is similar to that of the as-prepared. In order to magnetically decouple the dots of the $L1_0$ phase, the dots should be as much separated as possible. Since the TiN seed layer withstands the plasma etching for long time (minimum 220 s), the separation can be increased by increasing etching time without affecting the TiN remarkably! That allows the optimization of the nanopattern (size and separation of the dots). At present t=220 s was set together with the unchanged U_{DC}=1000 V and S=5.85 W/cm^2. Thus, the typical plan view SEM and XTEM images of the obtained nanopatterned $L1_0$ CoPt sample can be seen in Fig. 6(a) and Fig. 6(b), respectively.

The SEM in Fig. 6(a) shows that a pattern of well separated dots has been evolved. The hexagonal arrangement of the dots is almost defect free. According to low magnification SEM images not shown here, it consists of domains that extend to areas larger than 150 μm^2. On the other hand, all of the annealed sample surfaces seemed to be decorated with some contamination that couldn't be cleared away by acetone. This

residue is supposed to build up from CoPt clusters sputtered away by the Ar plasma re-deposited by magnetic attraction of the film.

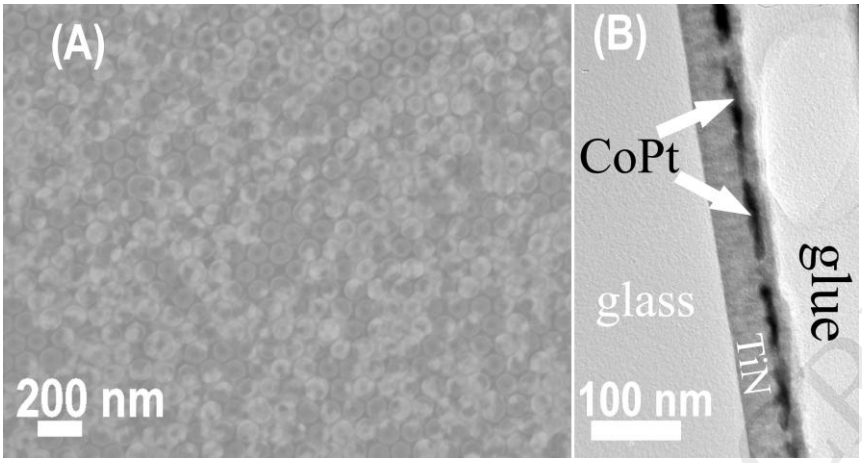

***Figure 6**. SEM (a) and XTEM (b) image of the patterned annealed ($L1_0$ phase) CoPt sample. The etching time was 220 s and U_{DC}=1000 V.*

In the XTEM (Fig. 6(b)), those re-deposited CoPt clusters mentioned above seem to appear superimposed on the pattern. (However, the flakes seem to overspread the pattern can be due to the electron beam not exactly perpendicular to the surface and due to some thinning artefact as well.) In sum, at the case of the annealed ($L1_0$) CoPt samples, the roughened and not completely coherent surface (see Fig. 2(a) and (b)) results in a pattern of rather non-uniform height and shape.

In order to avoid re-deposition provoked by magnetic attraction during RF plasma etching, the as-prepared (fcc) CoPt samples – that were first patterned – were subsequently annealed for 1 h at 700 °C in vacuum, below $2.5*10^{-6}$ mbar. This way, smooth and re-deposition free patterned $L1_0$ CoPt layers were fabricated. The typical plan view SEM, XTEM, and the HRXTEM of an $L1_0$ CoPt sample that was annealed after patterning are seen in Fig. 7(a), (b), and (c), respectively. An FFT of the HR image of the CoPt layer is represented on the right side of Fig. 7(c).

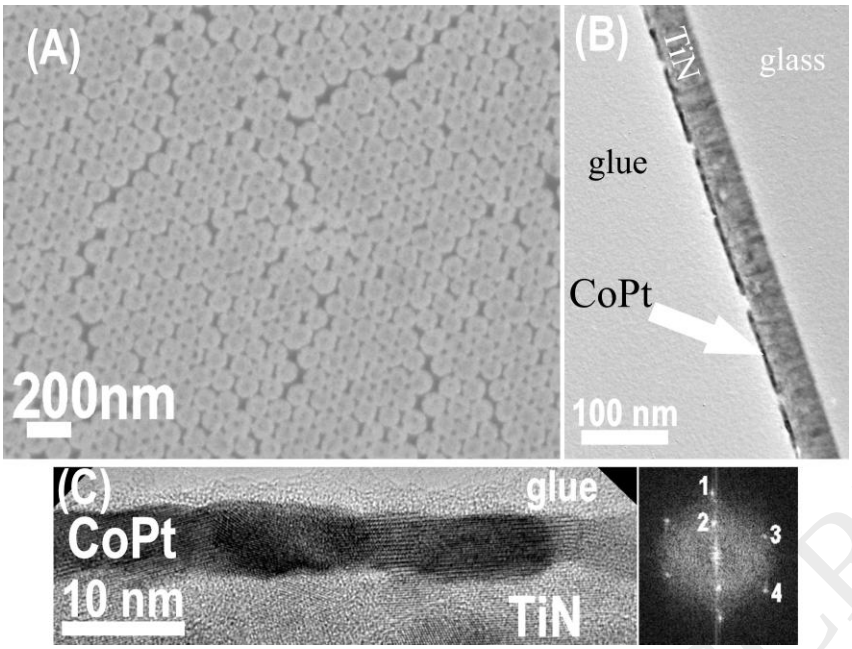

Figure 7*. SEM (a) and XTEM (b) image of an $L1_0$ CoPt sample that was annealed subsequent to patterning. (c): HRXTEM of the sample with an FFT insert of the HR image of CoPt layer. The marked reflections in the FFT are: 1 – fct CoPt(002); 2 – fct CoPt(001); 3 – fct CoPt(011); 4 – fct CoPt(110).*

The SEM image (Fig. 7(a)) shows the hexagonally ordered dots of the fct ($L1_0$) CoPt, and there is no sign of re-deposited matter. However, the disks are not as separated as in the case of Fig. 6(a), this is due to the shorter etching time of 100 s. Fig. 7(b) is the side view of the pattern of ~100 nm fct $L1_0$ CoPt disks. The HRXTEM image in Fig. 7(c), together with the FFT inset proves that annealing subsequent to patterning, also, results in the transition to fct ($L1_0$) CoPt phase with preferred [001] orientation. The reflections in the FFT denoted by numbers 1, 2, 3, and 4 refer to the lattice planes: fct CoPt(002) /1.849 Å/, fct CoPt(001) /3.684 Å/, fct CoPt(011) /2.185 Å/, and fct CoPt(110) /1.905 Å/, respectively.

3.3. Magnetic properties of the nanopatterned CoPt samples

The magnetic properties of the nanopatterned fct CoPt samples were measured by VSM. The typical M–H curve (relative magnetization as a function of the magnetic field) of

our samples is shown in Fig. 8(a). The patterned CoPt film clearly shows a strong perpendicular magnetic anisotropy. It can be seen that the in-plane direction is a hard axis and the perpendicular (out of plane) direction is the easy axis with a coercive force (H_c) as large as ~12 kOe. This result indicates that patterning on the present scale does not affect the perpendicular magnetic anisotropy originated from the magnetocrystalline anisotropy of the $L1_0$ structure. The curves in Fig. 8(a) are quite noisy that is due to both the low sensitivity of the available VSM and a small sample size (~1x0.5 cm^2 surface).

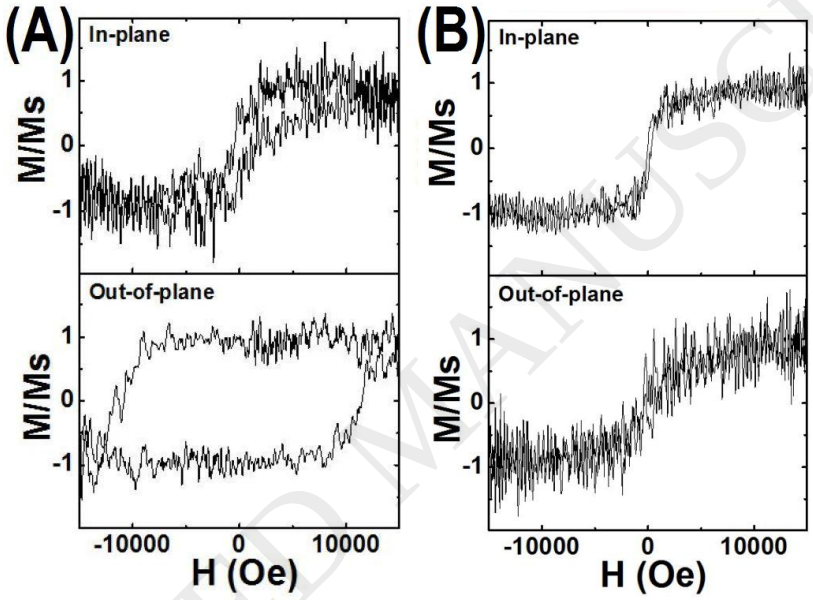

Figure 8. *(a) The typical M–H curve of our fct nanopatterned samples obtained by VSM. (b) The typical M–H curve of a patterned, but non-annealed CoPt sample obtained by VSM.*

In contrary, the typical M–H curve of the patterned but non-annealed CoPt films shown in Fig. 8(b) does not show significant hysteresis neither in plane nor out of plane direction. This is due to the disordered fcc phase; where there is no macroscopic anisotropy. Of course, this latter holds for the non-patterned and non-annealed CoPt thin films as well (e. g. [38]). It is to mention that the magnetic properties of the annealed but non-patterned CoPt films are described in the authors' previous paper [24]. Comparing the VSM result of the annealed but non-patterned CoPt film found in our

previous paper [24] with that of the nanopatterned and annealed CoPt sample (Fig. 8(a)), the two perpendicular measurements are very similar (besides the noise). The coercive force of the patterned CoPt samples seems to be somewhat larger, but this can't be stated due to the noise of the measurement. On the other hand, the in-plane hysteresis loop is way smaller in the case of the patterned sample.

Fig. 9 demonstrates a typical MFM image of a CoPt sample annealed after the patterning. It is to mention that the actual sample pieces used for the MFM measurements are different from those studied by the VSM (but identical in sense of fabrication process). The magnet employed for magnetizing the sample prior to MFM measurements can provide maximal external magnetic field up to 1.15 T, however that was not enough to saturate the sample as it can be deduced from Fig. 9 as well. (For comparison, a calculation had shown [39] that the write head has to apply ~2.4 T local field to switch a 1 Tbit/in^2 capacity dot-patterned media.) The yellow rings in Fig. 9 indicate the topographical pattern, and they are added from the topographical scan of the same area.

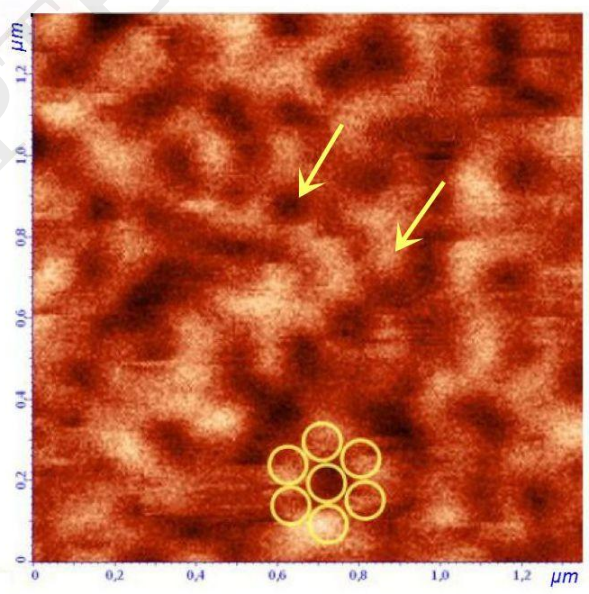

***Figure 9**. A typical MFM image of an fct CoPt layer annealed subsequent to nanopatterning taken at zero field after magnetizing by the field of 1.15 T. The yellow rings indicate the topographical patterns.*

Ideally, the MFM image should consist of either bright or dark contrast dots that exactly correspond to the topographical patterns. That is only slightly fulfilled here, due to the magnetic interaction between the dots. This magnetic coupling is the consequence of the short etching time of only 100 s that results in topographical pattern of not well separated dots.

However, Fig. 9 can be described as an MFM image that indicates dots showing either dark or bright contrast that means perpendicularly magnetized single domains as indicated by the arrows in the image. Besides those dots, there are areas where the magnetic domains expand to multiple (topographical) dots that supposed to be due to the magnetic coupling induced by the little separation among the dots. It is suggested that the magnetic coupling should decrease as the etching time is increasing (because the topographical separation increases between the edges of the dots) in an experiment carried out by annealing after the patterning process. Moreover, the topographical separation necessary to obtain single domain dots is decreasing with the decreasing feature size [40]. This is a promising phenomenon since the feature size of our nanopatterning technique can be decreased to 10-20 nm by decreasing the size of the applied nanospheres.

It is to mention that our MFM measurements taken of the samples annealed prior to patterning showed artefacts due to the previously mentioned re-depositied clusters that couldn’t be avoided. Thus, those are not included here.

4. Conclusions

This work has demonstrated, that nanopatterning by RF plasma etching through LB templates is appropriate for fabricating large area hexagonally ordered, ~100 nm sized dot arrays of CoPt. It was proven by TEM that, after annealing, the CoPt dots consist of ferromagnetic (fct) phase grains with [001] preferred orientation, and the transition from fcc to ferromagnetic fct ($L1_0$) phase occurs regardless of the order of annealing and patterning. It is, however, preferable to anneal the sample subsequent to nanopatterning, so that to avoid re-deposition of the etched away material due to magnetic attraction and obtain a patterned layer with dots of uniform thickness. The magnetic properties of the nanopatterned fct CoPt samples were revealed. According to VSM the fct nanopatterned samples exhibit broad, square-shape ferromagnetic hysteresis loop (with a coercive force of ~12 kOe) perpendicular to the surface. MFM measurements in external magnetic field have shown that the nanodots of the fct nanopatterned CoPt layers consist of single magnetic domains magnetized perpendicularly to the surface and there are domains that extend to multiple dots as well. Increased etching time that allows improving the separation of the dots of the pattern (together with reducing the dot size) is suggested to reduce the magnetic coupling between the dots.

The hexagonal nanopattern of ~100 nm ferromagnetic CoPt disks with magnetic easy axis perpendicular to the sample surface obtained in this work can be considered as a possibility to realize Bit Patterned Media. We suppose that the ~100 nm feature size can be reduced to a few tens of nanometers that is essential for high density media. The nanopatterning technique presented here is promising to be scaled up to industrial applications.

Acknowledgement

The authors are thankful to L. Illés for the contribution with the SEM investigations.

References

[1] Diana C. Leitao, Elvira Paz, Ana V. Silva, Anastasiia Moskaltsova, Simon Knudde, Francis L. Deepak, Ricardo Ferreira, Susana Cardoso, and Paulo P. Freitas, "Nanoscale Magnetic Tunnel Junction Sensing Devices With Soft Pinned Sensing Layer and Low Aspect Ratio," *IEEE Transactions on Magnetics*, vol. 50 (11), p. 4410508, 2014.

[2] M. Rahm, J. Bentner, J. Biberger, M. Schneider, J. Zweck, D. Schuh, and D. Weiss, "Hall-Magnetometry on Ferromagnetic Micro-Rhombs," *IEEE Transactions on Magnetics*, vol. 37 (4), pp. 2085-2087, 2001.

[3] P. J. Metaxas, M. Sushruth, R. A. Begley, J. Ding, R. C. Woodward, I. S. Maksymov, M. Albert, W. Wang, H. Fangohr, A. O. Adeyeye, and M. Kostylev, "Sensing magnetic nanoparticles using nano-confined ferromagnetic resonances in a magnonic crystal," *Applied Physics Letters*, vol. 106, pp. 232406 1-5, 2015.

[4] Chang Liu, Thomas Tsao, Yu-Chong Tai, Wenheng Liu, Peter Will, and Chih-Ming Ho, "A Micromachined Permalloy Magnetic Actuator Array for Micro Robotics Assembly Systems," *olid-State Sensors and Actuators, 1995 and Eurosensors IX. Transducers' 95. The 8th International Conference on*, vol. 1, pp. 328-331, 1995.

[5] Hyun Jin In, Hyungwoo Lee, Anthony J. Nichol, Sang-Gook Kim, and George Barbastathis, "Carbon nanotube–based magnetic actuation of origami membranes," *Journal of Vacuum Science & Technology B*, vol. 26, pp. 2509-2512, 2008.

[6] A. V. Chumak, V. I. Vasyuchka, A. A. Serga, and B. Hillebrands, "Magnon spintronics," *Nature Physics*, vol. 11, pp. 453-461, 2015.

[7] V. V. Kruglyak, S. O. Demokritov, and D. Grundler, "Magnonics," *Journal of Physics D: Applied Physics*, vol. 43, pp. 264001 1-14, 2010.

[8] V. Y. F. Leung, A. Tauschinsky, N. J. van Druten, and R. J. C. Spreeuw, "Microtrap arrays on magnetic film atom chips for quantum information science," *Quantum Information Processing*, vol. 10, pp. 955-974, 2011.

[9] A. Moser, K. Takano, D. T. Margulies, M. Albrecht, Y. Sonobe, Y. Ikeda, S. Sun, and E. E. Fullerton, "Magnetic Recording: Advancing into the Future," *Journal of Physics D: Applied Physics*, vol. 35, pp. R157–R167, 2002.

[10] O. Hellwig, A. Berger, T. Thomson, E. Dobisz, Z. Z. Bandic, H. Yang, and D. S. Kercher, "Separating dipolar broadening from the intrinsic switching field distribution in perpendicular patterned media," *Applied Physics Letters*, vol. 90, pp. 162516 1-3, 2007.

[11] T. Seki, T. Shima, K. Yakushiji, K. Takanashi , G. Q. Li, and S. Ishio, "Dot size dependence of magnetic properties in microfabricated L10-FePt (001) and L10-FePt (110) dot arrays," *Journal of Applied Physics*, vol. 100 (4), pp. 043915 1-8, 2006.

[12] B. D. Belle, F. Schedin, N. Pilet, T. V. Ashworth, E. W. Hill, P. W. Nutter, H. J. Hug, and J. J. Miles, "High resolution magnetic force microscopy study of e-beam lithography patterned Co⁄PtCo⁄Pt nanodots," *Journal of Applied Physics*, vol. 101 (9), pp. 09F517 1-3, 2007.

[13] Alongkorn Pimpin and Werayut Srituravanich, "Review on Micro- and Nanolithography Techniques and their Applications," *Engineering Journal*, vol. 16, pp. 37-55, 2012.

[14] Matthew C. Traub, Whitney Longsine, and Van N. Truskett, "Advances in nanoimprint lithography," *nnual review of chemical and biomolecular engineering*, vol. 7, pp. 583-604, 2016.

[15] Weimin Zhou, Jinhe Wang, Jing Zhang, Xiaoli Li, and Guoquan Min, "Large-area fabrication of 3D petal-like nanopattern for surface enhanced Raman scattering," *Applied Surface Science*, vol. 303, pp. 84–89, 2014.

[16] H. W. Deckman and J. H. Dunsmuir, "Natural Lithography," *Applied Physics Letters*, vol. 41, pp. 377-379, 1982.

[17] Pierre Colson, Catherine Henrist, and Rudi Cloots, "Nanosphere Lithography: A Powerful Method for the Controlled Manufacturing of Nanomaterials," *Journal of Nanomaterials*, vol. 2013 (ID:948510), pp. 1-19, 2013.

[18] S. L. Cheng, C. Y. Zhan, S. W. Lee, and H. Chen, "Enhanced formation of periodic arrays of low-resistivity NiSi nanocontacts on (0 0 1)Si0.7Ge0.3 by nanosphere lithography with a thin interposing Si layer," *Applied Surface Science*, vol. 257, pp. 8712– 8717, 2011.

[19] N. Nagy, Z. Zolnai, E. Fülöp, A. Deák, and I. Bársony, "Tunable ion-swelling for nanopatterning of macroscopic surfaces: The role of proximity effects," *Applied Surface Science*, vol. 259, pp. 331– 337, 2012.

[20] Wanchuan Xie, Jiang Chen, Lang Jiang, Ping Yang, Hong Sun, and Nan HuangKey, "Nanomesh of Cu fabricated by combining nanosphere lithography and high power pulsed magnetron sputtering and a preliminary study about its function," *Applied Surface Science*, vol. 283, pp. 100– 106, 2013.

[21] János Szívós, Miklós Serényi, Szilárd Pothorszky, András Deák, Gábor Vértesy, and György Sáfrán, "A technique for nanopatterning diverse materials," *Surface & Coatings*

Technology, vol. 313, pp. 115–120, 2017.

[22] Werner Stöber, Arthur Fink, and Ernst Bohn, "Controlled growth of monodisperse silica spheres in the micron size range," *Journal of Colloid and Interface Science*, vol. 26 (1), pp. 62-69, 1968.

[23] Daniel K. Schwartz, "Langmuir-Blodgett film structure," *Surface Science Reports*, vol. 27 (7-8), pp. 245–334, 1997.

[24] Hongyu An, Jian Wang, János Szívós, Takashi Harumoto, Takumi Sannomiya Sannomiya, Shinji Muraish, György Sáfrán, Yoshio Nakamura, and Ji Shi, "Perpendicular coercivity enhancement of CoPt/TiN films by nitrogen incorporation during deposition," *Journal of Applied Physics*, vol. 118, pp. 203907 1-4, 2015.

[25] András Deák, Erzsébet Hild, Attila Lajos Kovács, and Zoltán Hórvölgyi, "Contact angle determination of nanoparticles: film balance and scanning angle reflectometry studies," *Physical Chemistry Chemical Physics*, vol. 9, pp. 6359–6370, 2007.

[26] András Deák, B. Bancsi, Attila Lajos Tóth, Attila Lajos Kovács, and Zoltán Hórvölgyi, "Complex Langmuir–Blodgett Films from Silica Nanoparticles: An Optical Spectroscopy Study," *Colloids and Surfaces A: Physicochemical and Engineering Aspects*, vol. 278, pp. 10-16, 2006.

[27] J. C. Woolley, J. H. Phillips, and J. A. Clark. (2017, Mar.) Crystallography Open Database. [Online]. http://www.crystallography.net/cod/1525472.html?applet=jsmol

[28] H. J. Beattie and F. L. VerSnyder, "Microconstituents in high temperature alloys," *Transactions of the American Society for Metals*, vol. 45, pp. 397-428, 1953.

[29] Atomwork. (2017, Mar.) Inorganic Material Database. [Online]. http://crystdb.nims.go.jp/index_en.html

[30] János L. Lábár, "Electron Diffraction Based Analysis of Phase Fractions and Texture in Nanocrystalline Thin Films, Part I: Principles," *Microscopy and Microanalysis*, vol. 14 (4), pp. 287-295, 2008.

[31] János L. Lábár, "Electron Diffraction Based Analysis of Phase Fractions and Texture in Nanocrystalline Thin Films, Part II: Implementation," *Microscopy and Microanalysis*, vol. 15 (1), pp. 20-29, 2009.

[32] János L. Lábár, "Electron Diffraction Based Analysis of Phase Fractions and Texture in Nanocrystalline Thin Films, Part III: Application Examples," *Microscopy and Microanalysis*, vol. 18 (3), pp. 406-420, 2012.

[33] János L. Lábár, "Consistent indexing of a (set of) SAED pattern(s) with the

ProcessDiffraction program," *Ultramicroscopy*, vol. 103, pp. 237-249, 2005.

[34] Petros I. Stavroulakis, N. Christou, and D. Bagnall, "Improved deposition of large scale ordered nanosphere monolayers via liquid surface self-assembly," *Materials Science and Engineering B*, vol. 165, pp. 186–189, 2009.

[35] Y. Xia, Y. Yin, Y. Lu, and J. McLellan, "Template-Assisted Self-Assembly of Spherical Colloids into Complex and Controllable Structures," *Advanced Functional Materials*, vol. 13 (12), pp. 907–918, 2003.

[36] William D. Sproul and Robert Rothstein , "High Rate Reactively Sputtered TiN Coatings on High Speed Steel Drills," *Thin Solid Films*, vol. 126, pp. 257-263, 1985.

[37] Marc Wittmer, "Properties and microelectronic applications of thin films of refractory metal nitrides," *Journal of Vacuum Science & Technology A*, vol. 3, pp. 1797-1803, 1985.

[38] Kevin R. Coffey, Michael A. Parker, and J. Kent Howard, "High Anisotropy L10 Thin Films for Longitudinal Recording," *IEEE Transactions on Magnetics*, vol. 31 (6), pp. 2737-2739, 1995.

[39] Sharat Batra, Jonathan D. Hannay, Hong Zhou, and Jason S. Goldberg, "Investigations of perpendicular write head design for 1 Tb/in2," *IEEE transactions on magnetics*, vol. 40 (1), pp. 319-325, 2004.

[40] Naganivetha Thiyagarajah, Mohamed Asbahi, Rick T. J. Wong, Kendrick W. M. Low, Nikolai L. Yakovlev, Joel K. W. Yang, and Vivian Ng, "A facile approach for screening isolated nanomagnetic behavior for bit-patterned media," *Nanotechnology*, vol. 25, pp. 225203 (1-6), 2014.

Figure
Click here to download high resolution image

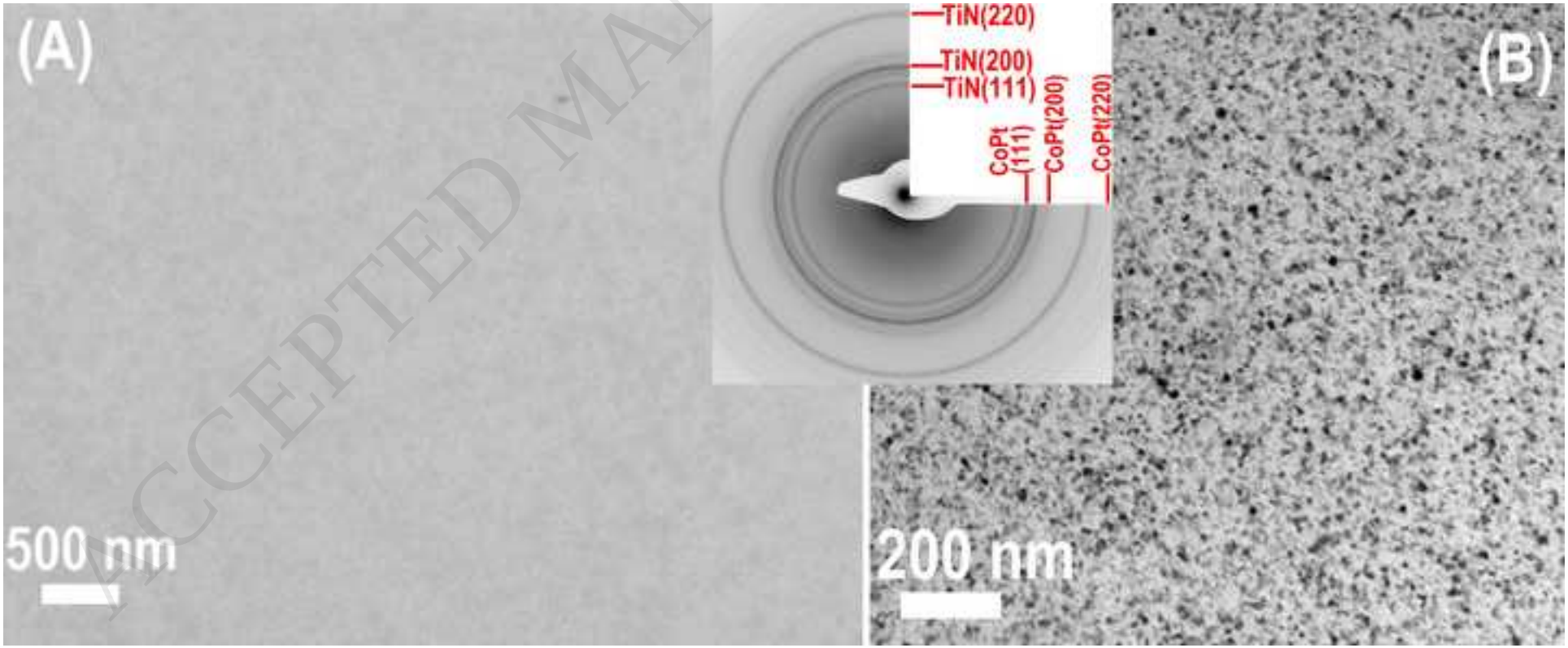

Figure 2 A and 2 B

Click here to download high resolution image

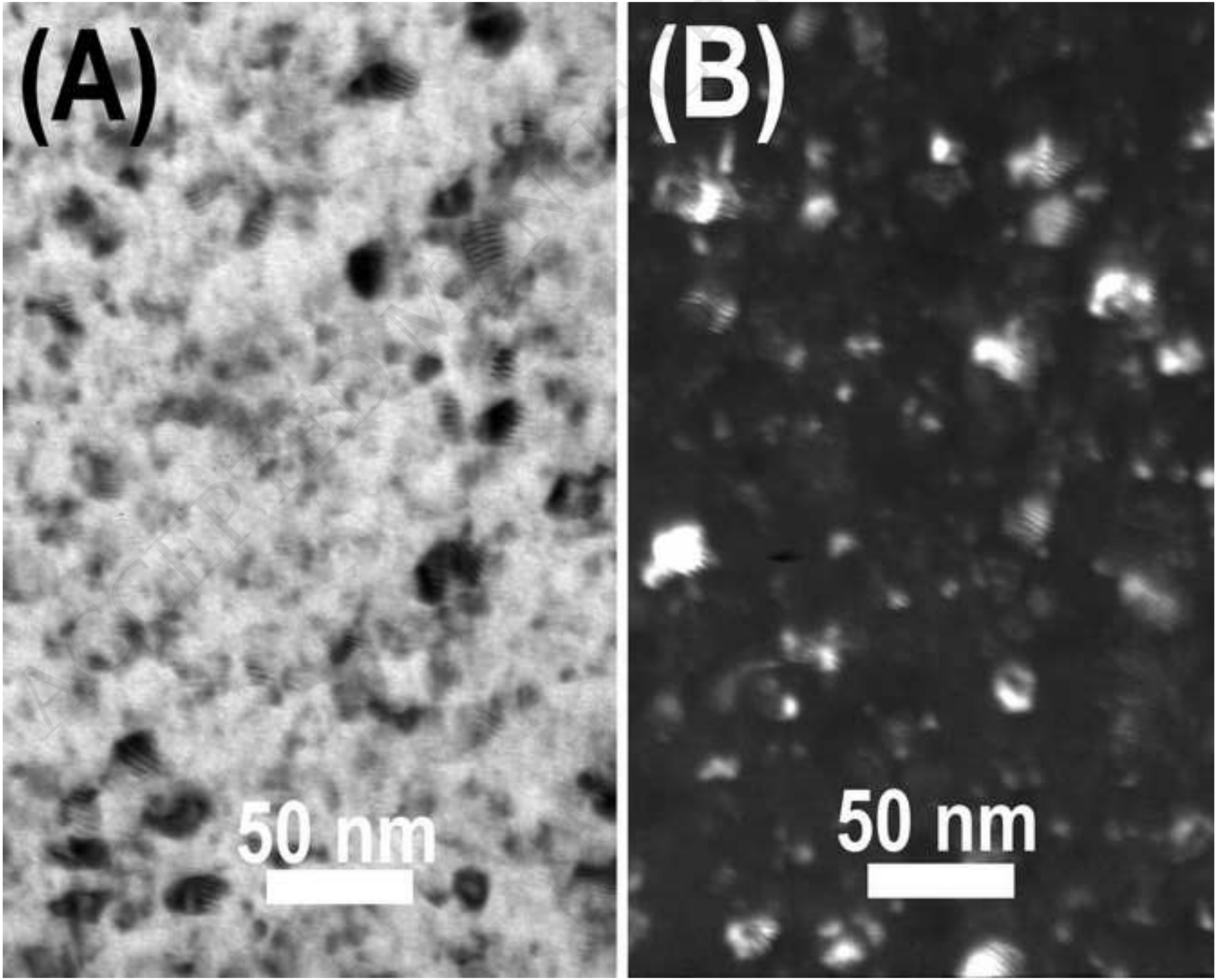

Figure 2 C and 2 D

Click here to download high resolution image

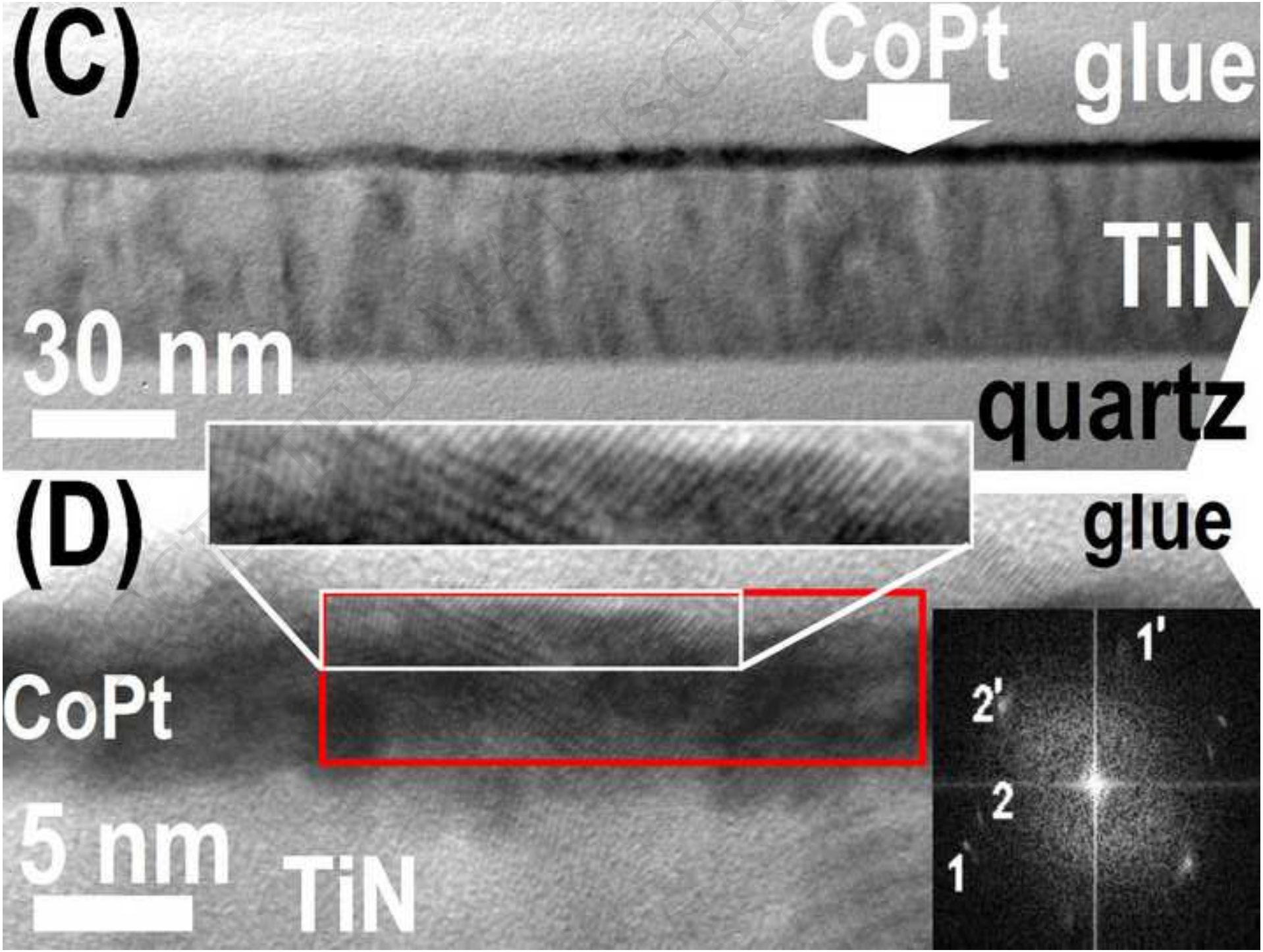

Figure 3

Click here to download high resolution image

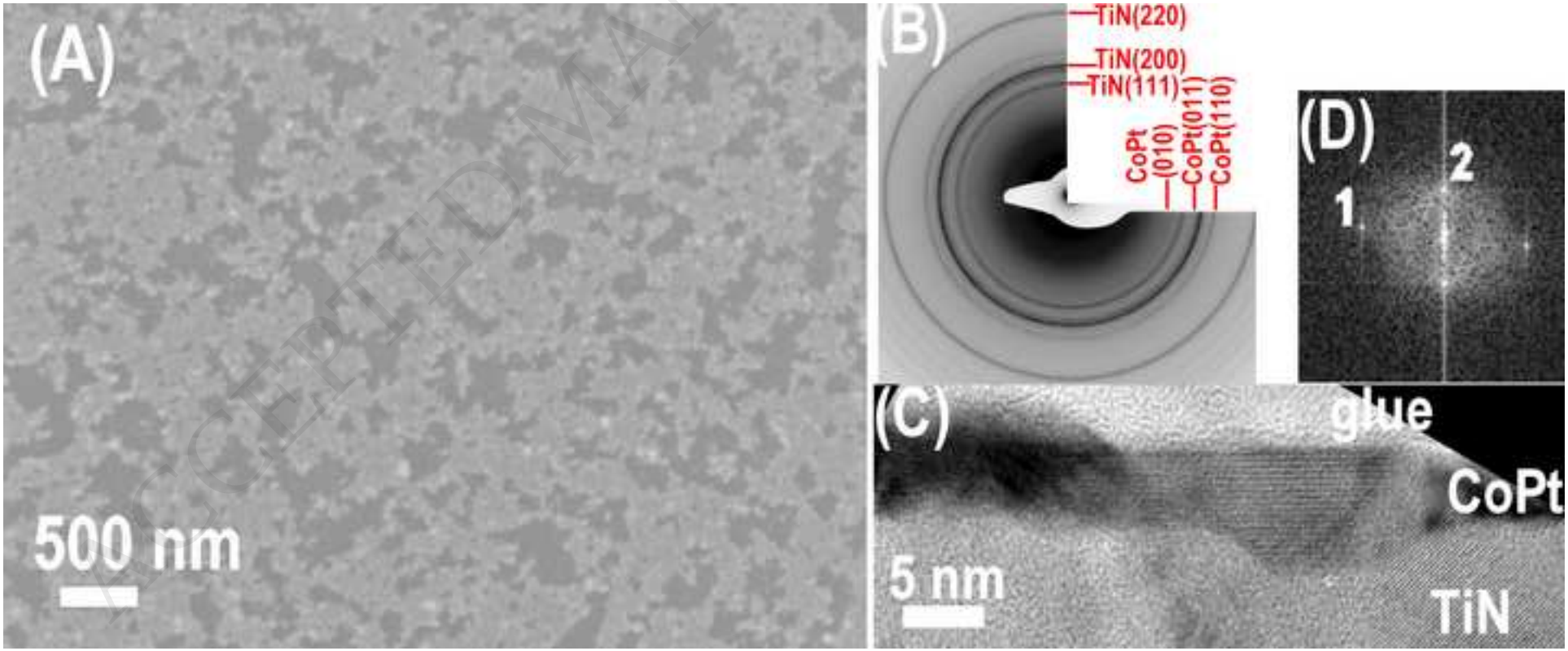

Figure 4

Click here to download high resolution image

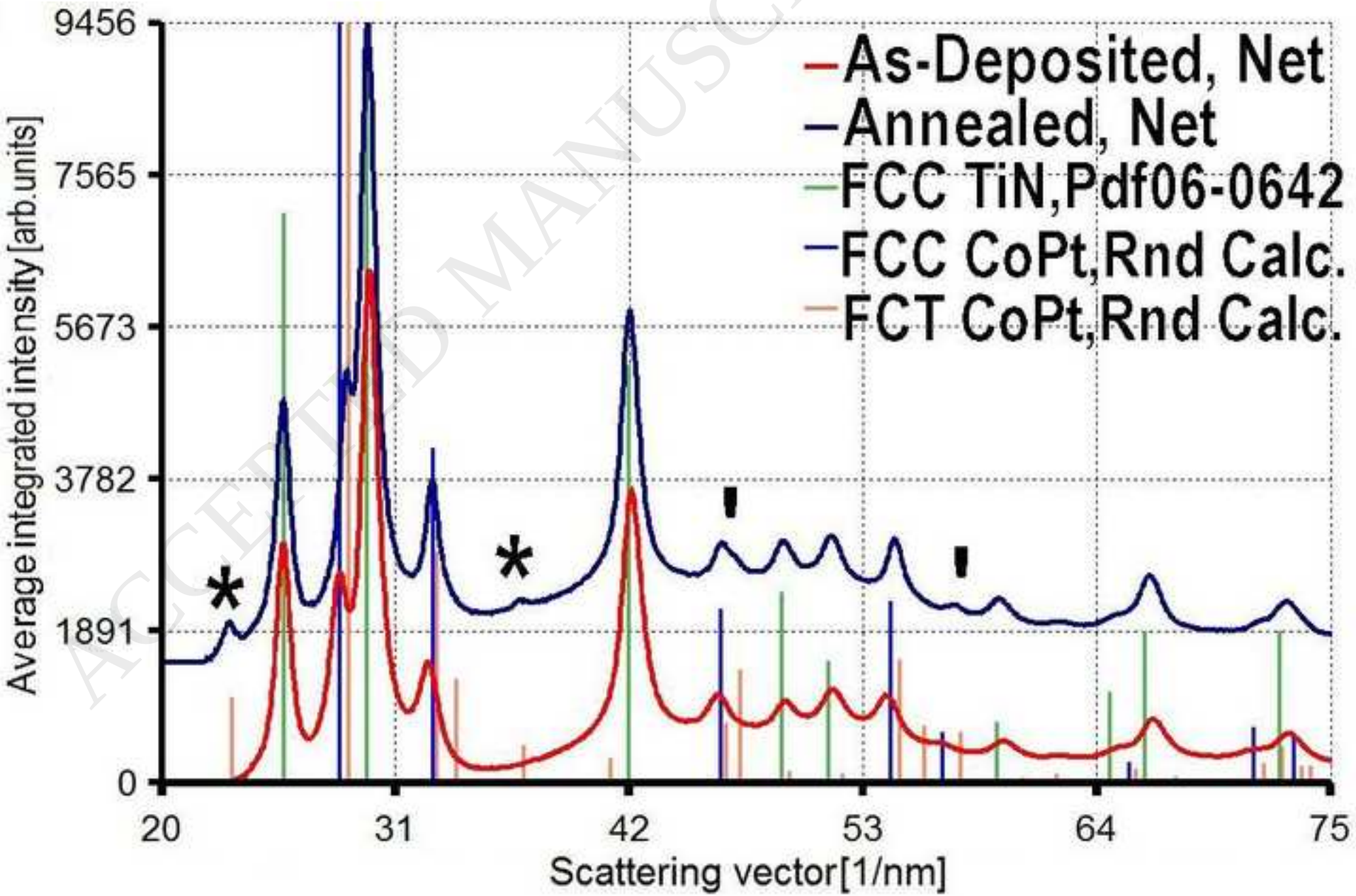

Figure 5
Click here to download high resolution image

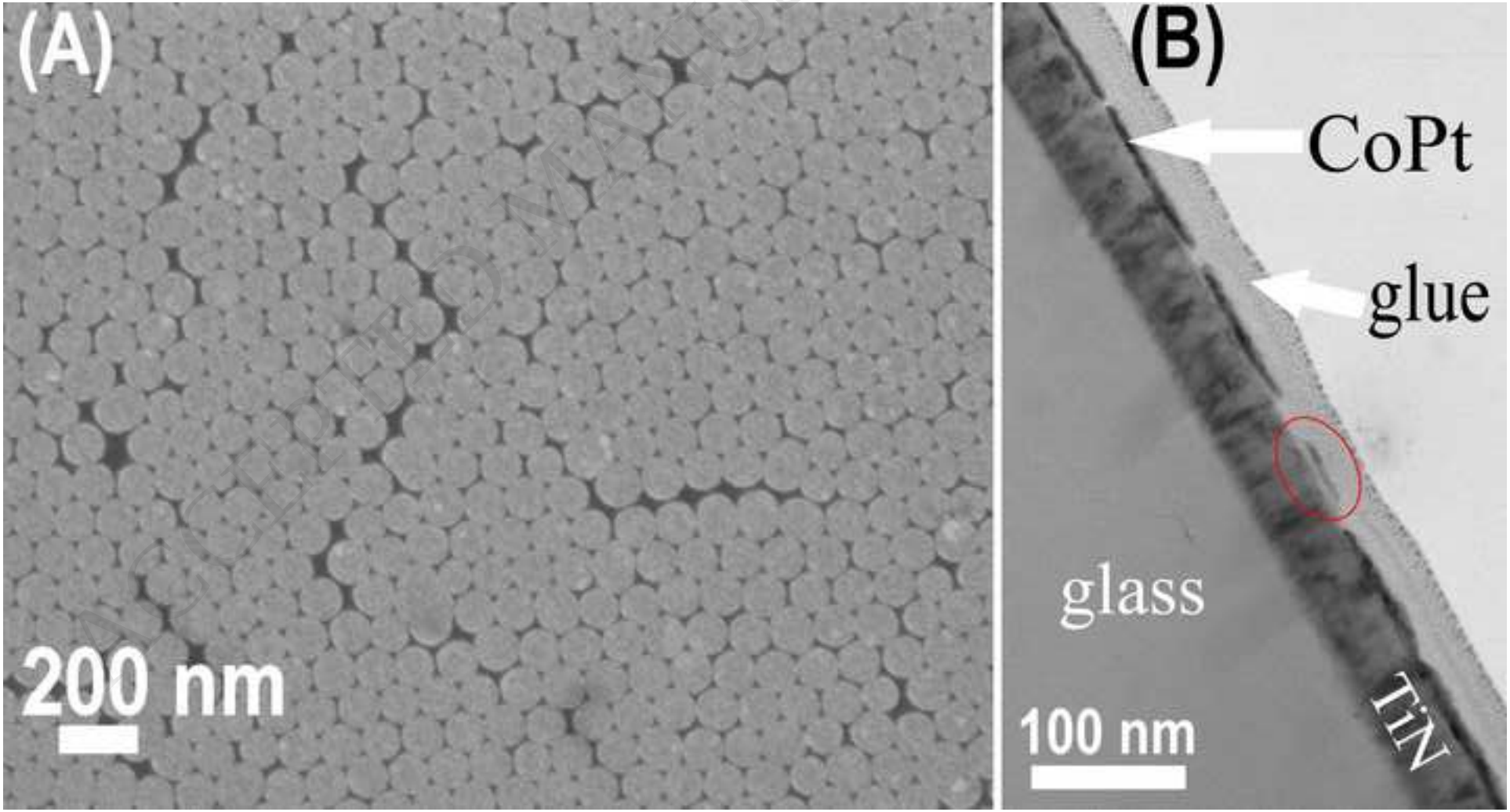

Figure 6
Click here to download high resolution image

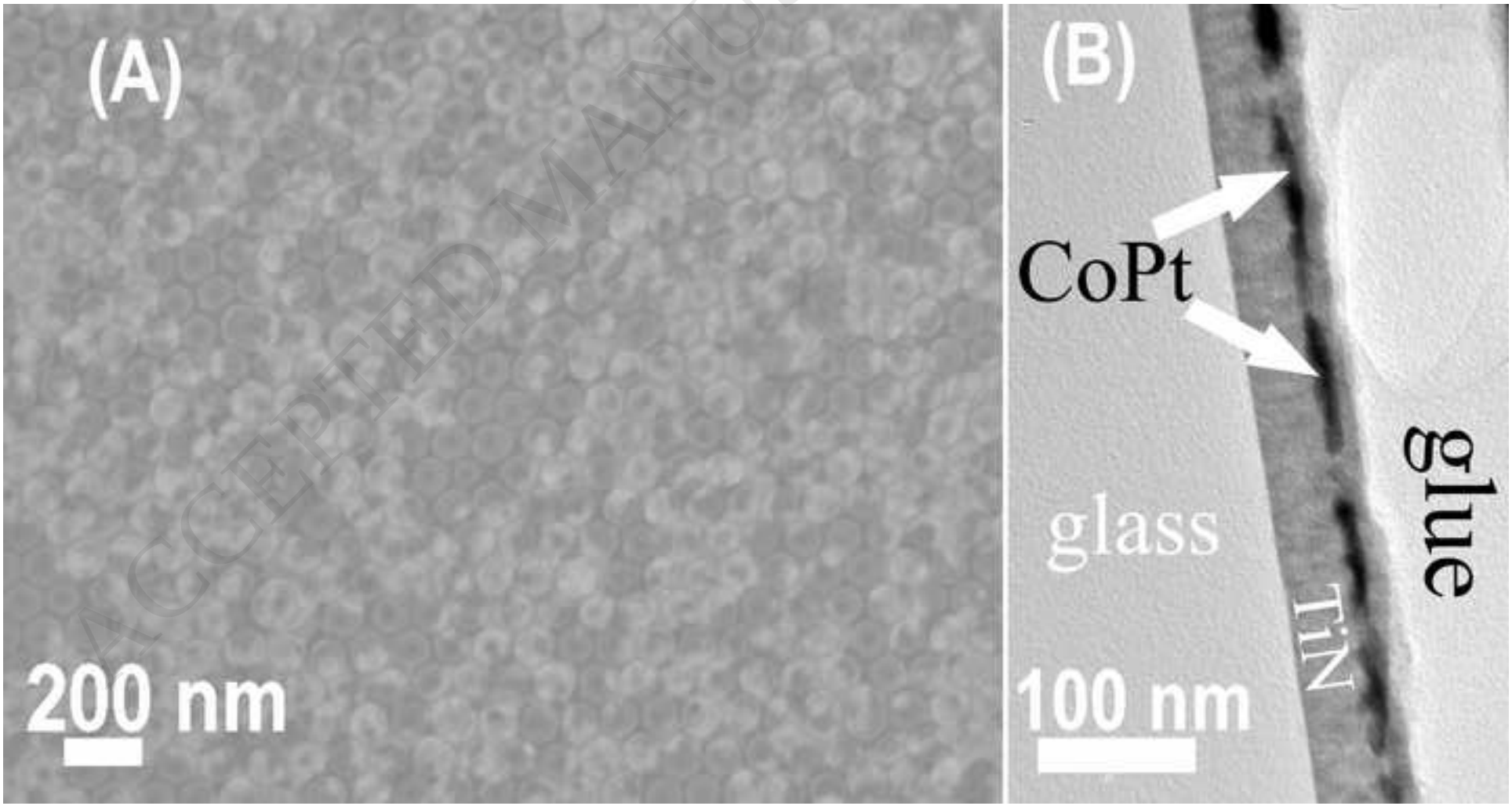

Figure 7

Click here to download high resolution image

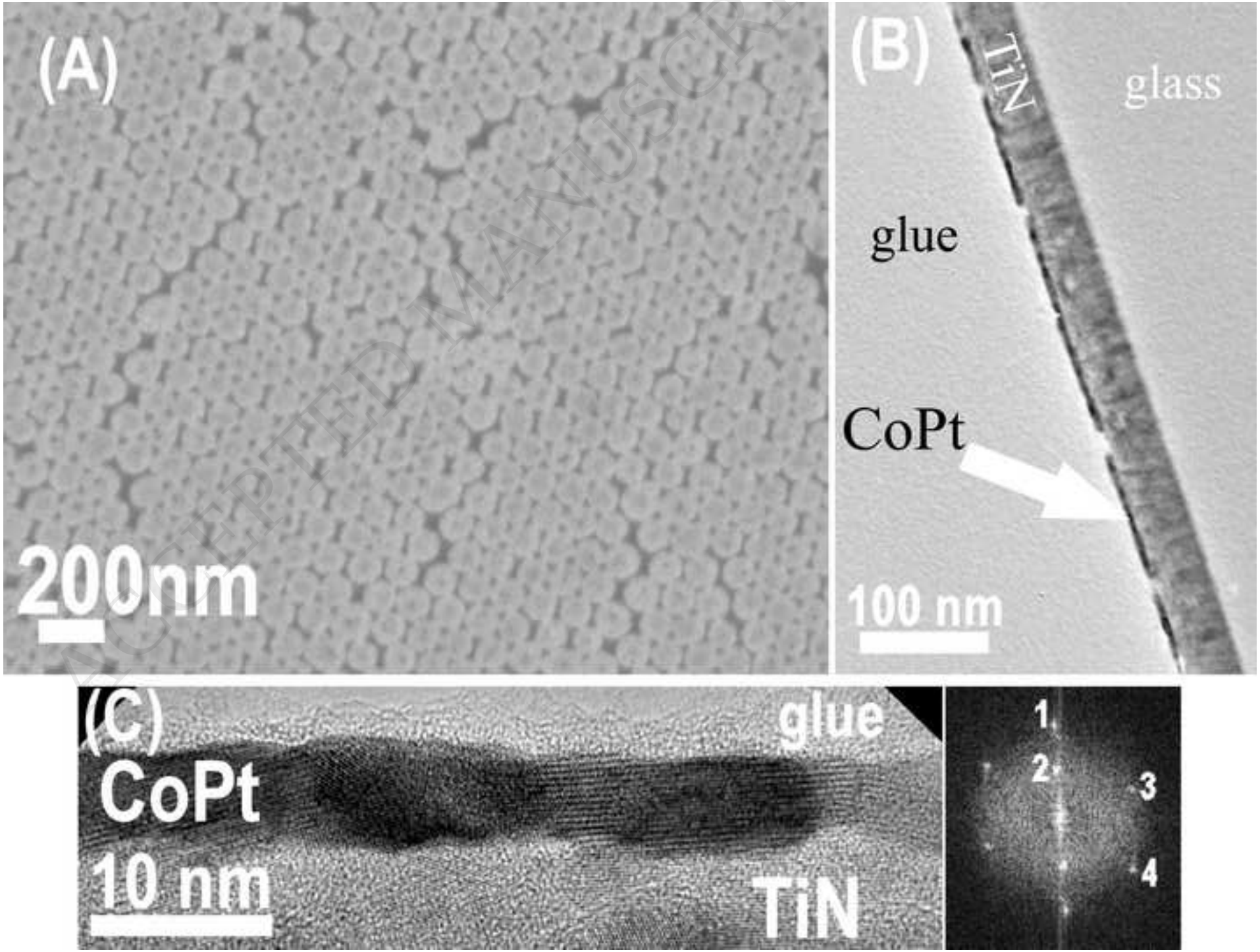

Figure 8

Click here to download high resolution image